

Design and fabrication of novel three-dimensional multi-electrode array using SOI wafer

Huai-Yuan Chu^a, Tzu-Ying Kuo^a, Baowen Chang^b, Shao-Wei Lu^c,
Chuan-Chin Chiao^{c,d}, Weileun Fang^{a,b,*}

^a Department of Power Mechanical Engineering, National Tsing Hua University, Taiwan

^b MEMS Institute, National Tsing Hua University, Taiwan

^c Institute of Molecular Medicine, National Tsing Hua University, Taiwan

^d Department of Life Sciences, National Tsing Hua University, Taiwan

Received 23 May 2005; received in revised form 1 February 2006; accepted 1 February 2006

Available online 23 March 2006

Abstract

A novel method has been developed for the manufacture of a three-dimensional multi-electrode array (3D MEA), particularly, the shape of micro-tips can be varied by MEMS technology to construct different multi-electrode array. It improved the disadvantage of single electrode, which meant that it was available for multi-recording and analysis of a series of signals. Overcoming the difficulty of making interconnection line on 3D MEA chips via innovative fabrication process design. Using local isolation and removal of oxide films to forming electrodes and interconnections with oxide isolation covers. A 10×10 3D MEA with a distance of $100 \mu\text{m}$ between each other for further bio-neural signals was demonstrated, and a test on rabbit retina was also available. Besides, integrating pre-amplifier and built-in resistors with 3D MEA was brought out to hopefully increase the efficiency of sensing.

© 2006 Elsevier B.V. All rights reserved.

Keywords: 3D Multi-electrode array; Recording of retinal neurons; SOI wafer

1. Introduction

The response of single neuron is traditionally recorded by a glass or a metal electrode. In last decade, many attempts have been made to design and fabricate multi-electrode arrays (MEAs) in order to measure the responses of multiple neurons simultaneously. These MEAs not only can drastically increase the efficiency of neural recordings [1,2], they can also allow neuroscientists to investigate synchronous firing by a population neurons in retina [2–4], visual cortex [5], somatosensory cortex [6], and hippocampus [7]. These correlated firing patterns in the network of a neural system are keys to understand the flow of information in the brain [8]. In addition, development of MEAs may facilitate the design of the neural interface for the cortical vision prosthesis [9]. Since the dimension of neural systems under investigation usually range from several tens

to several hundred micrometers, the number of the electrode and the spacing between the electrodes should be easily adjusted to fit different applications. Hence, the microelectrode array made using semiconductor technology is extremely suitable for the development of MEA.

In the past, the semiconductor process has been extensively employed to fabricate the micro multi-electrodes. For instance, the lithography technique is applied to implement the in-plane multi-electrode array [10]. Thus multi-signals can be recorded simultaneously to realize the spatiotemporal relationship among cells. However, the planar electrode in [4] is only several microns thick, and cannot penetrate into the tissue. Hence, the MEA with insertion capability was presented in [11–14] to facilitate the recordings in the deeper neurons.

In the recent years, the MEMS technology gradually plays an important role for the fabrication of three-dimensional MEA. The micromachined 3D MEA with better insertion ability has been realized in [7,15]. Applying the planar fabrication technology to integrate needle electrodes with various heights on Si wafer has also been considered in [16]. However, the needle

* Corresponding author. Tel.: +886 3 5742923; fax: +886 3 5739372.

E-mail address: fang@pme.nthu.edu.tw (W. Fang).

tip of the 3D MEA is not sharp by using the processes such as LIGA [17], or electroplating [18,19], thus it may damage the tissue. In most applications, a needle electrode is preferred to penetrate the layered tissue, and form a good contact between the probe tip and the neuron for improving the resolution of the bio-electrical sensing signals.

The present study has successfully demonstrated simple fabrication processes to implement a novel 3D MEA. The processes can monolithically integrate the needle electrodes with signal lines and bond pads of the 3D MEA on a single chip. Thus, some complicated assembly processes can be prevented. Moreover, the combination of pre-amp on chip to reduce the noise coupling was also realized. The present MEA design is flexible and easy made to fit any required dimension, and use only silicon without metal material. These features are important for developing MEA device to explore various neural tissues.

2. Concept and fabrication processes

This study employed the SOI wafer to manufacture the 3D MEA and then monolithically integrating with signal lines. A schematic drawing of the 3D MEA is illustrated in Fig. 1. Briefly, the 3D MEA was consisted of the needle electrode, signal line, bonding pad, isolation wall, and footing resistor. This section will bring out several design considerations about the 3D MEA in Fig. 1; in addition, the fabrication processes will also be discussed.

2.1. Design concept

The SOI wafer with low resistivity device silicon layer was employed in the present study. This device silicon layer formed the electrodes and signal lines, so that components with two different thickness were required by the process, as shown in Fig. 1. The thickness of the device layer was mainly determined by the

height H of the needle electrode. A sharp tip was designed to enable the needle electrode to pierce into tissue easily. The whole needle electrode except the tip was covered with insulation layer to prevent from noise coupling. The needle tip acted as the signal input port of the device. Moreover, an auxiliary structure named footing resistor was designed to prevent the undercutting problem during ICP etching process. The footing resistor was a Si structure added around the base of MEA.

The signal line acted as electrical interconnection between the needle electrode and bond pad. The height h of the signal line was mainly determined by the impedance of the device. In this study, the signal line and the needle electrode were located on the same side of the wafer. Thus, the insulation layer was also employed to isolate signal lines from each other, so as to reduce the noise. Moreover, the insulation oxide layer of the SOI wafer was also used to prevent the cross-talk of the signal lines. The bond pads acted as the output port of the 3D MEA after wire bonding. The feature of the bond pad in this study was a mesa. The presented fabrication process would implement the bond pads monolithically using the device layer, as indicated in Fig. 1. A better electrical transfer rate will be available for the pad after coated with a metal layer

2.2. Process flow

Fig. 2 shows the fabrication processes employed in this study to realize the multi-electrodes illustrated in Fig. 1. The fabrication processes began with a low resistivity SOI wafer. The processes needed only three masks. In Fig. 2(a) and (b), the SOI wafer was etching by ICP twice to define the heights of the signal line and electrode. The conductivity of signal line was determined by the resistivity of SOI wafer. The shape and height of micro-tip could be varied to meet different requirements by combination of isotropic, anisotropic etching, and ICP deep etching. The process in Fig. 2(a) also pre-defined the pattern of the signal lines before the ICP deep silicon etching. Thus, the photolithography on a complicated surface topology as shown in Fig. 2(b) was prevented. Moreover, the distance between signal lines, the size of bond pad, and the geometry of microelectrode were precisely defined by the ICP etching. Fig. 2(c) shows that thermal oxidation was used to provide the isolation layer for the needle electrode and its signal line. Since the top surface of the electrodes were protected by Si_3N_4 , the thermal oxide was only covered the sidewall of the electrodes and the surface of the signal line. After removing the Si_3N_4 film, the silicon on the needle tip would be exposed. Thus bulk silicon etching techniques could be employed to define the tip profile of the needle. For instance, Fig. 2(d) indicates the dry isotropic Si etching by XeF_2 . Other available techniques include the wet anisotropic etching by TMAH and KOH, and wet isotropic etching by HNA. The thermal oxide on top of the bonding pad was grown in the process of Fig. 2(a), however, the thermal oxide for side wall protection was grown in the process of Fig. 2(c). In this study, the thickness of the thermal oxide in Fig. 2(c) was thicker than that in Fig. 2(a). If properly control the etching time, the thinner thermal oxide on top of the bond pad could be fully stripped after dipping the wafer in HF, as shown in Fig. 2(e). However,

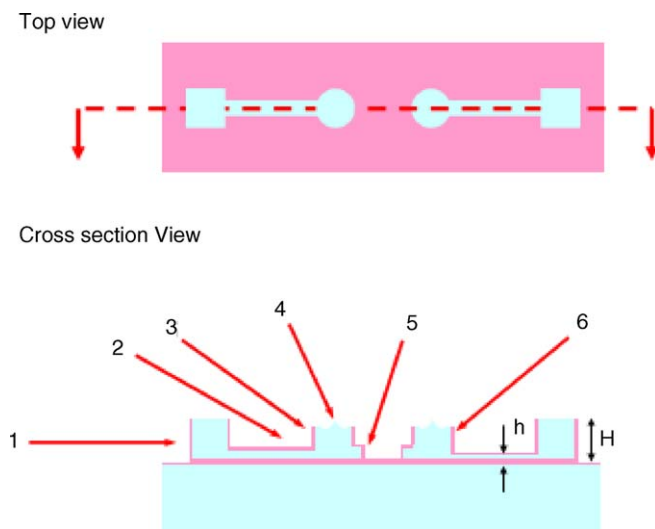


Fig. 1. A schematic view of the cross-section of 3D MEA, components of device including (1) bonding pad, (2) signal line, (3) needle electrode, (4) needle tip, (5) footing resistor, and (6) insulation layer.

(a) Thin film deposition and pattern



(b) 2-step ICP etching



(c) Local oxidation

(d) XeF₂ etching

(e) Local oxide removal

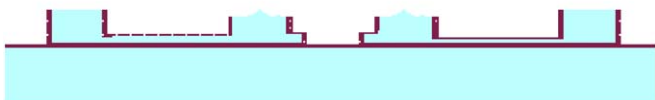


Fig. 2. Illustrations of the process flow.

the sidewall of the needle and the signal line remained protected by the thicker thermal oxide.

3. Fabrication and results

According to aforementioned fabrication processes, the 3D MEA was realized. Moreover, the concept of on-chip integration with other electronics components, such as pre-amp, was also demonstrated. This section will show details of fabrication results. In this study, the dimension of prototype electrode design was based on the ganglion cell of the retina of rabbits. Thus, the height of the needle tip was less than $7\ \mu\text{m}$ in this design, and the height of the needle electrode was ranging from 50 to $70\ \mu\text{m}$. This design ensured that tissue would be inserted around the target cell. The diameter of needle tip is preferred to be smaller than $2\ \mu\text{m}$ for neural application.

3.1. Multi-electrode array

The SEM photo in Fig. 3(a) shows a 10×10 MEA monolithically integrating with signal lines and bond pads. Fig. 3(b)

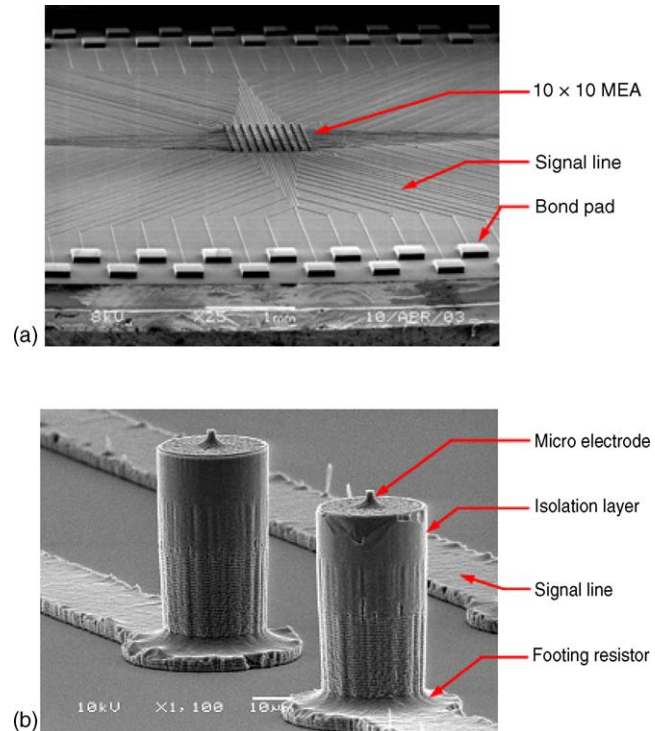


Fig. 3. The SEM photo of typical fabrication results: (a) a 10×10 MEA, and (b) the close-up view of the 3D MEA.

shows the close-up view of two 3D electrodes. Components of 3D multi-electrode, such as needle electrode, needle tip, signal line, footing resistor, and isolation wall, are clearly observed. The electrode is approximate $60\ \mu\text{m}$ high and $30\ \mu\text{m}$ wide and covered with a $2\ \mu\text{m}$ thick SiO_2 isolation layer. In addition, the electrode has a micro-tip with $7\ \mu\text{m}$ high and less than $2\ \mu\text{m}$ wide. The distance between the adjacent needles is $100\ \mu\text{m}$. The shape and height of micro-tip was tuned by etching process, as shown in Fig. 4(a) and (b). The isotropic etching via XeF_2 gas was employed to fabricate the tips in Fig. 4(a). The diameter of needle tip was below $100\ \text{nm}$. However, if the electrode was etched by ICP before XeF_2 isotropic etching, the aspect ratio of the tip would be increase, as shown in Fig. 4(b). The diameter of needle tip became $2\ \mu\text{m}$, moreover, the tip size could be tuned by etching time.

3.2. Integrated with pre-amp

For neural applications, the signal to noise ratio could be too small to distinguish the real signal from unwanted one. A pre-amp was exploited in this study to improve the signal condition. Moreover, this study decreased the pathway of interconnection between the pre-amp and the needle electrodes to avoid the disturbance of noise. Fig. 5 shows the 3D MEA with a pre-amp glued to the bonding stage. The pre-amp is an unpackaged die of LMC660 MDA manufactured by National Semiconductor Corporation. In Fig. 5, the resistors were exploited to tune the amplification ratio of the pre-amp, and the bonding stage supplied a path to electrical ground. The fabrication processes for the device in Fig. 5 were compatible with the processes in Fig. 2.

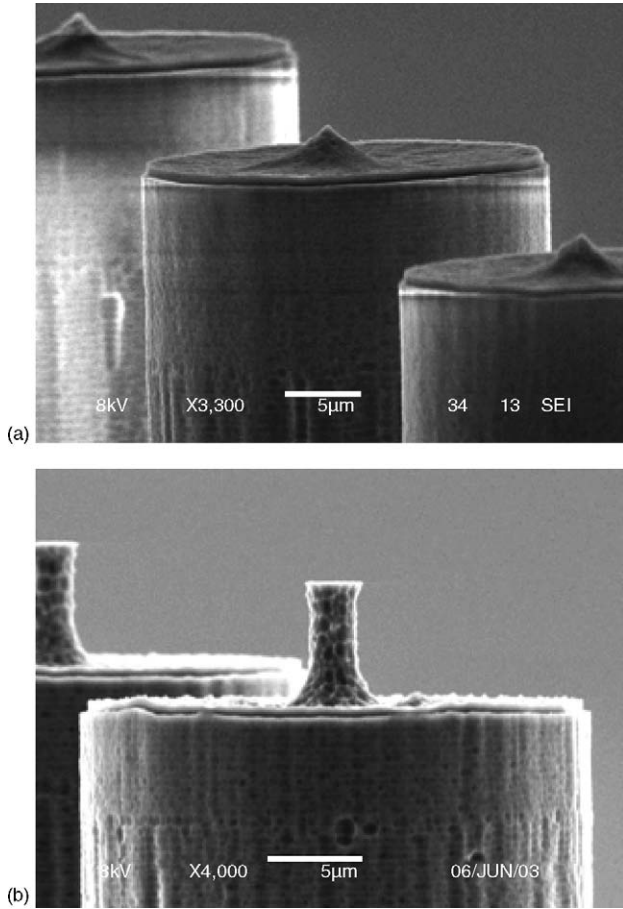


Fig. 4. Different shape and height of needle tip: (a) tips etched by XeF₂ gas, and (b) tips etched by ICP plus XeF₂ etching.

Thus, the bonding stage, resistors, and signal lines were fabricated simultaneously using the presented processes.

3.3. Packaging and system integration

The side view of the whole packaged 3D MEA system is shown in Fig. 6. The system consisted of a culture chamber, the 3D MEA, and various electrical interconnections. The test biological sample was placed in electrolyte inside the culture

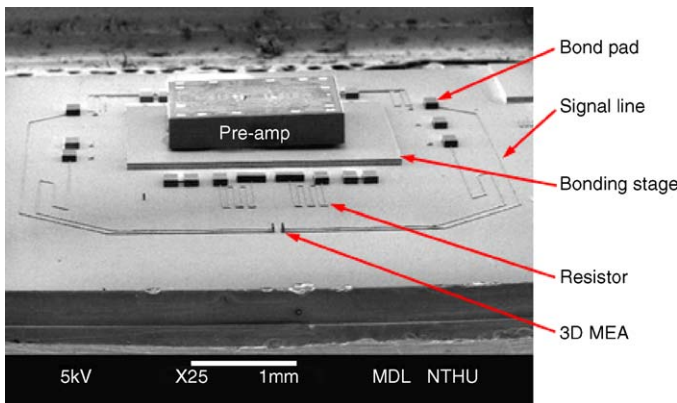


Fig. 5. The SEM photo of the 3D MEA integrating with a pre-amp.

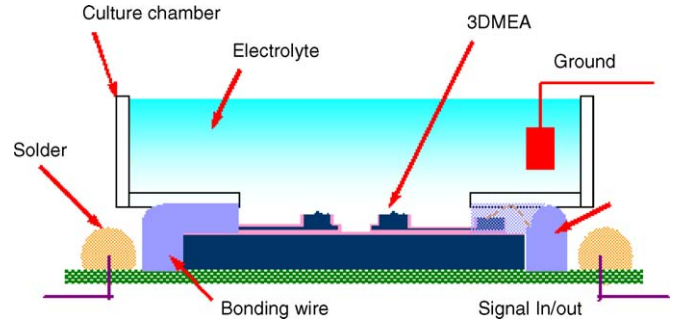


Fig. 6. Schematic illustration of a packaged 3D MEA.

chamber. To package the device, the chip with 3D MEA was firstly glued to a printed circuit board (PCB) using anaerobic adhesive, and then baking on hot plate at 150 °C for 10 min. The wire bond was used to connect the pads on PCB and chip. The photo in Fig. 7(a) shows the wire bonding of a 2 × 2 MEA chip

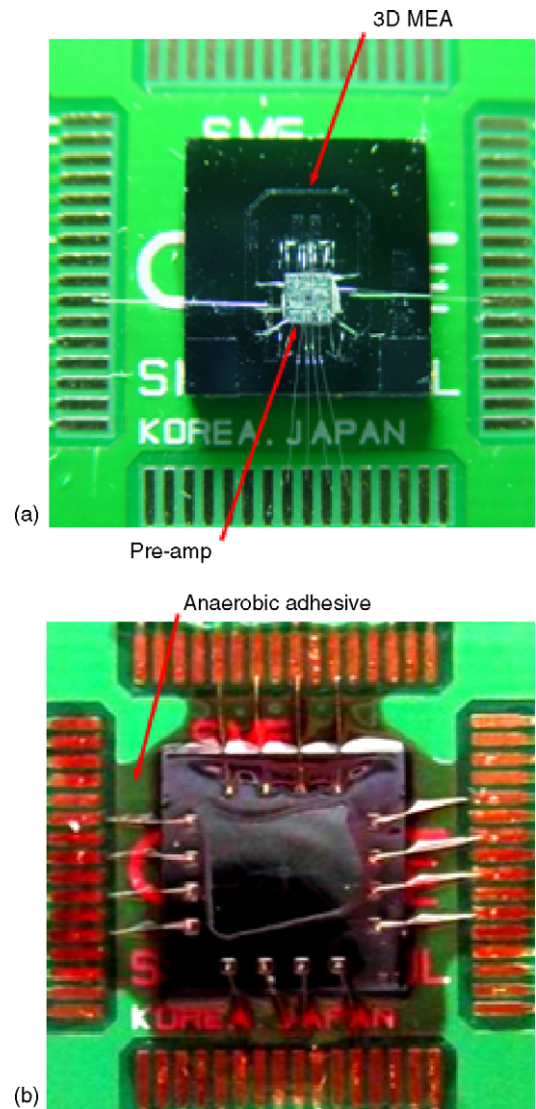


Fig. 7. Photos of (a) the wire bonding of a 2 × 2 MEA chip with a pre-amp chip and the PCB, and (b) the protection of wires after covering with epoxy encapsulation.

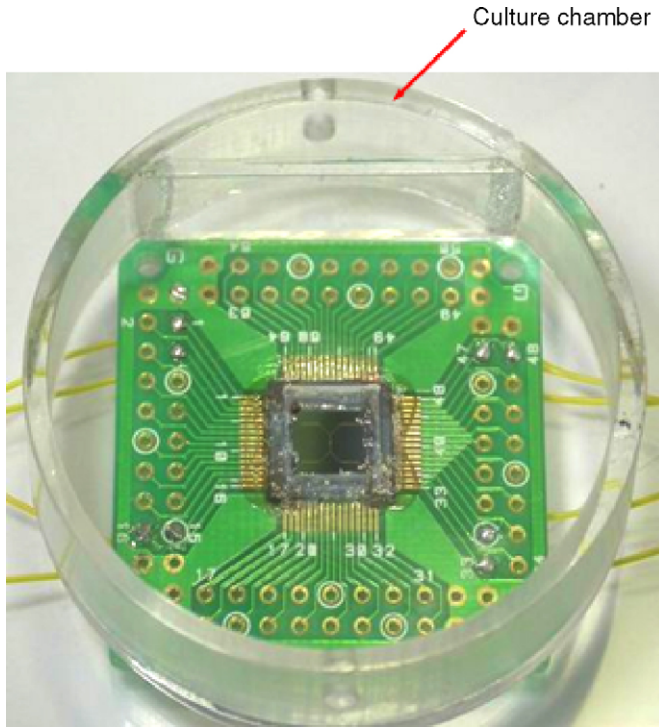


Fig. 8. The culture chamber of a 2×2 MEA system.

with a pre-amp chip and the PCB. The bonding wires were also protected by covering anaerobic adhesive or epoxy and solidified on hot plate. This provided moisture and electrical isolation from environment. The photo in Fig. 7(b) shows the 4×4 MEA covered with anaerobic adhesive. Fig. 8 shows the packaged 2×2 MEA system after the aforementioned assembly and packaging steps. Thus, the device was isolated when immersing in electrolyte except the tips for multi-neural recordings.

4. Testing

The 3D MEA has been evaluated by the qualitatively observation of the features in Figs. 3 and 4. The present device was also evaluated based on its electrical performances, including the insulation of the sidewall and the impedance of the MEA. Therefore, to evaluate the capability of the 3D MEA, an isolated rabbit retina was used in testing.

4.1. Insulation of the sidewall

One of the primary merits of the presented 3D MEA was local oxidation to provide insulations of electrodes and transmission lines. This design can prevent the coupling of noise from environment through electrodes and the signal line during test. The insulation wall is qualitatively observed in Fig. 9. After the specimen was over-etched by XeF_2 , the silicon was over etched from top of the electrode. Thus, only the insulation wall made of oxide was left. Moreover, this study employed the electroplating technique to further demonstrate the performance of electrical isolation. The nickel electroplating was used in the

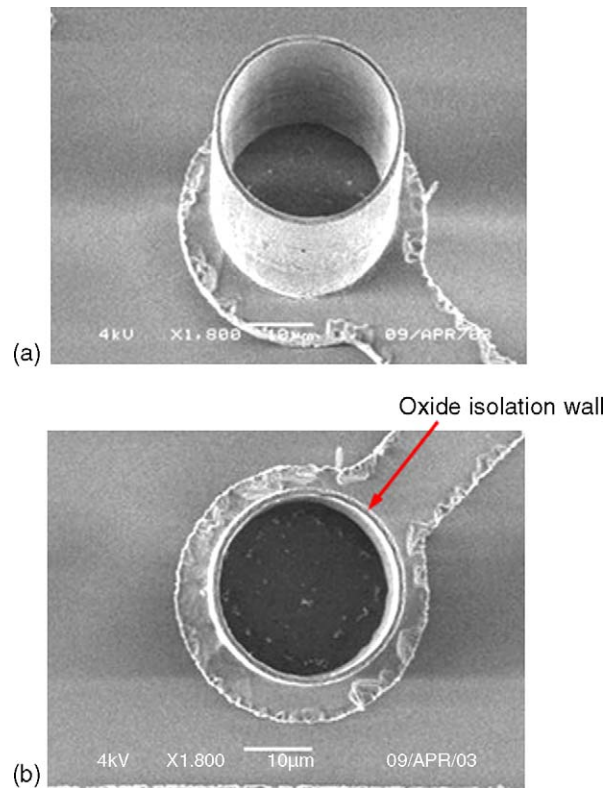


Fig. 9. The SEM photos of isolation wall after the silicon inside was etched away: (a) the bird's-eye view of isolation wall, and (b) top view of the isolation wall.

experiment. The SEM photo in Fig. 10(a) shows the electrodes before electroplating. After electroplating for several seconds, the nickel was only plated on the tip of electrodes, as shown in Fig. 10(b), and no metal was on insulation wall and signal line. Hence, it shows that the top surface is the only conductive region of the electrode.

4.2. Impedance measurement

The impedance of MEA has to properly match with that of amplifier to improve the measured signal condition. The experiment setup in Fig. 11(a) was employed to determine the impedance of electrodes. The test setup consisted of a packaged 3D MEA system shown in Fig. 6 and an impedance measurement instrument. After pouring 1 M KCl electrolyte into the culture chamber in Fig. 8, the 3D MEA was immersed into the solution. The resistance of electrodes determined from the resistivity ($0.01 \Omega \text{ cm}$) and the dimensions of 3D MEA was ranging from 10 to $20 \text{ k}\Omega$. Fig. 11(b) shows the measured impedances of the 3D MEA after tested with a sinusoidal voltage source (100 mV, and $10\text{--}10^3 \text{ Hz}$). The impedance decreased as the frequency of the AC signal increased. The impedance was approximately $14 \text{ k}\Omega$ with a phase of -60° , when the frequency was 10 Hz. As the frequency increased to 1 kHz, the impedance decreased to $4 \text{ k}\Omega$ with a phase of -13° . It shows that the impedance of the present needle electrode was suitable for recording the ganglion cell of the retina of rabbits.

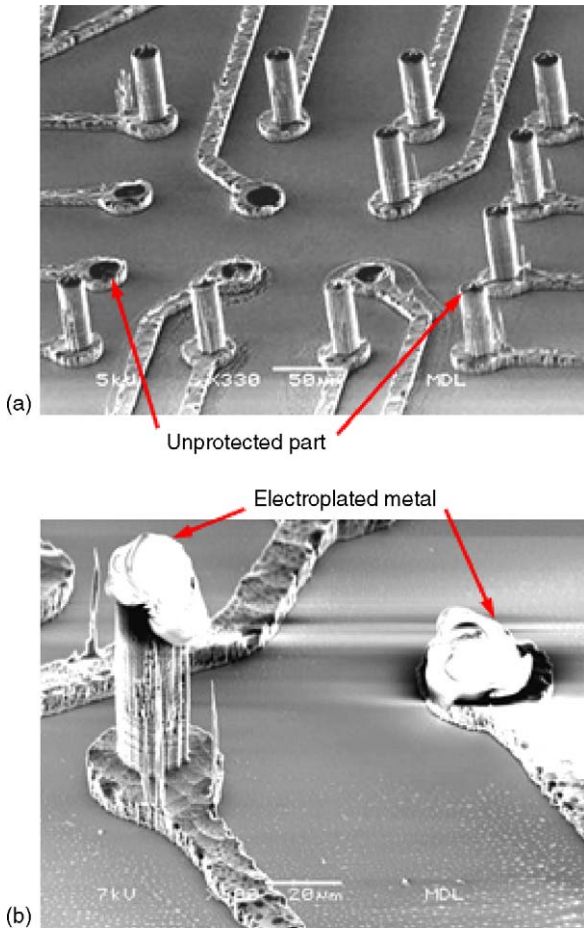


Fig. 10. Photos of isolation wall: (a) before electroplating test, and (b) metal deposited onto conductive surface after electroplating.

4.3. Recording of retinal neurons

The ultimate goal of making this 3D MEA is to record biological signals. To evaluate the capability of the 3D MEA, an isolated rabbit retina was used in testing. Detailed preparation of rabbit retina for electrophysiological recording is described in [20]. The isolated rabbit retina was placed onto the 3D MEA (ganglion cell side down), and the whole assembly (Fig. 8) was mounted on the stage of an upright fluorescence microscope (Axioskop 2 Plus FS, Zeiss, Germany). Since one channel extracellular amplifier (ISO-80, WPI, USA) was used in testing, only a single electrode can be connected to the amplifier each time to record the neuronal signals directly. The analog signals were converted to digital signals and stored in a PC computer via the DAQ card and the interface supported by LabVIEW (National Instruments, USA). A typical spontaneous response of retinal ganglion neurons is shown in Fig. 12. It appears that more than one ganglion cells fired spontaneously. Since the impedance is low in this 3D MEA, and a retina piece with higher cell density was used in this recording, it is likely that multiple cells were monitored simultaneously. In future, it would be desirable to design the MEA with higher impedance, so that a single unit recording can be achieved. Several electrodes of the 3D MEA

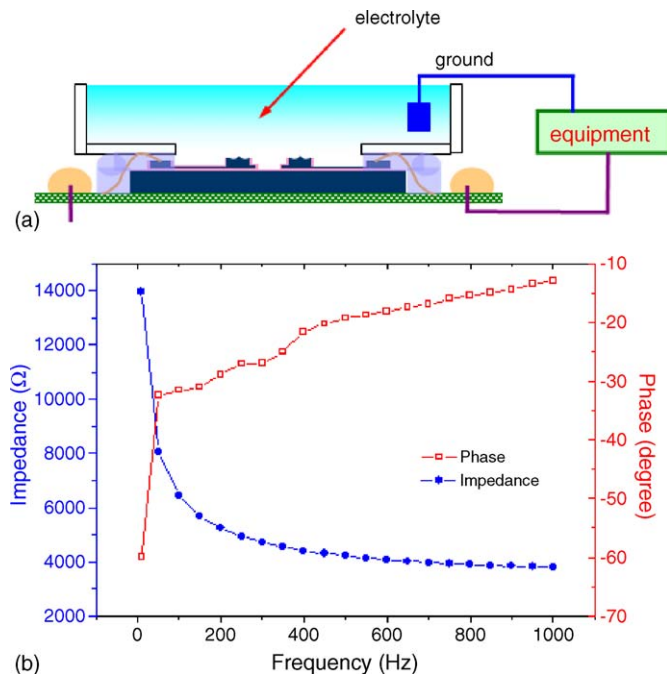


Fig. 11. Impedance measurement: (a) the experiment setup, and (b) the measurement results.

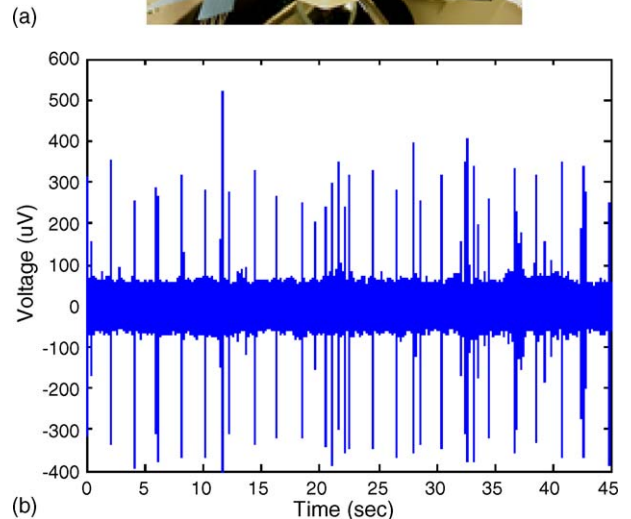
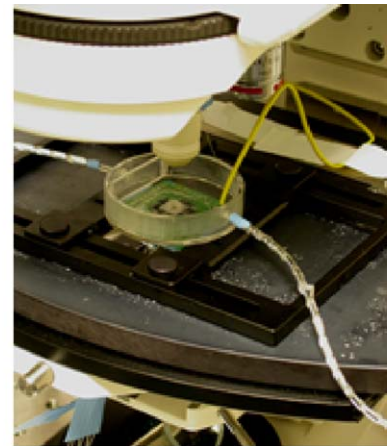


Fig. 12. (a) Experiment setup, and (b) spontaneous responses of retinal ganglion neurons recorded from a single electrode of the 3D MEA.

have been individually tested. The results were generally consistent among the electrodes in the 3D MEA.

5. Conclusion

A novel three-dimensional multi-electrode array (3D MEA) for bio-medical applications, such as neural recording, has been demonstrated. A three-mask process based on SOI wafer was developed to not only realize a 10×10 array of multi-height electrodes but also monolithically integrate the electrodes with signal lines and bond pads. The electrodes and signal lines were covered with a $2 \mu\text{m}$ thick SiO_2 isolation layer to reduce the noise by the local oxidation process. A sharp needle tip was designed and fabricated on top of the electrode, thus the damage of cells during recording was remarkably reduced. The impedance of each electrode met the neural signal requirement. And a typical response of retinal ganglion neurons was also demonstrated. Besides, this study also integrated the pre-amp and built-in resistors with 3D MEA to increase the S/N ratio.

Acknowledgements

The authors would like to thank the Brain Research Center and the Nano- and Micro-manufacturing lab of National Tsing Hua University, the Central Regional MEMS Research Center of National Science Council, the Semiconductor Research Center of National Chiao Tung University, and the National Nano Device Laboratory, for providing the neural recording and the fabrication facilities.

References

- [1] E.J. Chichilnisky, D.A. Baylor, Receptive-field microstructure of blue–yellow ganglion cells in primate retina, *Nat. Neurosci.* 2 (1999) 889–893.
- [2] S.H. DeVries, Correlated firing in rabbit retinal ganglion cells, *J. Neurophysiol.* 81 (1999) 908–920.
- [3] M. Meister, L. Lagnado, D.A. Baylor, Concerted signaling by retinal ganglion cells, *Science* 270 (1995) 1207–1210.
- [4] I.H. Brivanlou, D.K. Warland, M. Meister, Mechanisms of concerted firing among retinal ganglion cells, *Neuron* 20 (1998) 527–539.
- [5] D.J. Warren, E. Fernandez, R.A. Normann, High-resolution two-dimensional spatial mapping of cat striate cortex using a 100-microelectrode array, *Neuroscience* 105 (2001) 19–31.
- [6] R.S. Petersen, M.E. Diamond, Spatial-temporal distribution of whisker-evoked activity in rat somatosensory cortex and the coding of stimulus location, *J. Neurosci.* 20 (2000) 6135–6143.
- [7] M.O. Heuschkel, M. Fejt, M. Raggenbass, D. Bertrand, P. Renaud, A three-dimensional multi-electrode array for multi-site stimulation and recording in acute brain slices, *J. Neurosci. Methods* 114 (2002) 135–148.
- [8] E. Salinas, T.J. Sejnowski, Correlated neuronal activity and the flow of neural information, *Nat. Rev. Neurosci.* 2 (2001) 539–550.
- [9] R.A. Normann, E.M. Maynard, P.J. Rousche, D.J. Warren, A neural interface for a cortical vision prosthesis, *Vision Res.* 39 (1999) 2577–2587.
- [10] U. Egert, B. Schlosshauer, S. Fennrich, W. Nisch, M. Fejt, T. Knott, T. Muller, H. Hammerle, A novel organotypic long-term culture of the rat hippocampus on substrate-integrated multielectrode arrays, *Brain Res. Protoc.* 2 (1998) 229–242.
- [11] N.A. Blum, B.G. Carkhuff, H.K. Charles, R.L. Edwards, R.A. Meyer, Multisite microprobes for neural recordings, *IEEE Trans. Biomed. Eng.* 38 (1991) 68–74.
- [12] J. Ji, K.D. Wise, An implantable CMOS circuit interface for multiplexed microelectrode recording arrays, *IEEE J. Solid-State Circ.* 27 (1992) 433–443.
- [13] G. Ensell, D.J. Banks, D.J. Ewins, W. Balachandran, P.R. Richards, Silicon-based microelectrodes for neurophysiology fabricated using a gold metallization/nitride passivation system, *J. Microelectromech. Syst.* 5 (1996) 117–121.
- [14] C. Xu, W. Lemon, C. Liu, Design and fabrication of a high-density metal microelectrode array for neural recording, *Sens. Actuators A* 96 (2002) 78–85.
- [15] P.K. Campbell, K.E. Jones, R.J. Huber, K.W. Horch, R.A. Normann, A silicon-based, three-dimensional neural interface: manufacturing processes for an intracortical electrode array, *IEEE Trans. Biomed. Eng.* 38 (1991) 758–768.
- [16] P. Griss, P. Enoksson, H.K. Tolvanen-Laakso, P. Merilainen, S. Ollmar, G. Stemme, Micromachined electrodes for biopotential measurements, *J. Microelectromech. Syst.* 10 (2001) 10–16.
- [17] J.A. Bielen, W.L.C. Rutten, A.W. Schmidt, R. Weiel, Fabrication of multi-electrode array structures for intra-neural stimulation: assessment of the LIGA method, in: *Engineering in Medicine and Biology Society, Amsterdam, Netherlands, 1996*, pp. 268–269.
- [18] A. Hung, D. Zhou, R. Greenberg, J.W. Judy, Micromachined electrodes for retinal prostheses, in: *Proceedings of the IEEE-EMBS Special Topic Conference on Microtechnologies in the Medicine and Biology, Madison, Wisconsin, May, 2002*, pp. 76–79.
- [19] A. Hung, D. Zhou, R. Greenberg, J.W. Judy, Micromachined electrodes for high density neural stimulation systems, in: *Proceedings of the MEMS'02, Las Vegas, Nevada, January, 2002*, pp. 56–59.
- [20] C.-C. Chiao, R.H. Masland, Starburst cells non-directionally facilitate the responses of direction selective retinal ganglion cells, *J. Neurosci.* 22 (2002) 10509–10513.

Biographies

Huai-Yuan Chu was born in Taipei, Taiwan 1977. He received his MS and PhD degree in Power Mechanical Engineering Department, National Tsing Hua University, Taiwan, in 2002 and 2005 respectively. His current research interests include MEMS applications in printing systems, CNT-MEMS and micro bio-system for neural recording.

Tzu-Ying Kuo was born in Taipei, Taiwan, in 1978. He received his Master degree from Power Mechanical Engineering Department of National Tsing Hua University in 2003. Currently he is working in Industrial Technology Research Institute (ITRI), Taiwan. His current research focus on system in package, such as 3D packaging and integral substrate with embedded chips.

Baowen Chang was born in Tainan, Taiwan, in 1980. She received her Master degree from Institute of Microelectromechanical System of National Tsing Hua University in 2004. Currently she is working in Nano Technology Integration Department of Taiwan Semiconductor Manufacturing Company, Ltd., Taiwan. Her current works focus on nano technology projects and taking care of products.

Shao-Wei Lu was born in Taoyuan, Taiwan, in 1980. He received his BS degree from Department of Physics, National Tsing Hua University in 2004. Currently he is studying for the Master degree in Institute of Molecular Medicine, National Tsing Hua University, Taiwan. His current research interests in the information coding of the rabbit retinal ganglion cells.

Chuan-Chin Chiao was born in Taipei, Taiwan, in 1969. He received his PhD degree from University Maryland in 2000. His doctoral research focused on determining spectral properties of natural scenes and their effects on animal eye design. In 2000, he worked as a postdoctoral research at Harvard Medical School. He joined the Life Science Department at the National Tsing Hua University (Taiwan) in 2002, where he is now an assistant professor as well

as a faculty of Molecular Medicine Institute. His research interests include retina neurobiology, vision science, and behavioral neuroscience.

Weileun Fang was born in Taipei, Taiwan, in 1962. He received his PhD degree from Carnegie Mellon University in 1995. His doctoral research focused on the determining of the mechanical properties of thin films using

micromachined structures. In 1995, he worked as a postdoctoral research at Synchrotron Radiation Research Center, Taiwan. He is currently an associate professor at Power Mechanical Engineering Department, National Tsing Hua University, Taiwan. His research interests include MEMS with emphasis on microoptical systems, microactuators and the characterization of the mechanical properties of thin films.